

Supporting Information

Cosolvents Restrain Self-Assembly of a Fibroin-like Peptide on Graphite

Robert Ccorahua, Hironaga Noguchi, and Yuhei Hayamizu.*

Department of Materials Science and Engineering, School of Materials and Chemical
Technology, Tokyo Institute of Technology, Tokyo 152-8550, Japan.

Sample preparation

As depicted in Fig. 1b, we prepared samples as following. Flakes of graphite (Asbury Carbons, USA) and MoS₂ were transferred onto a silicon wafer with a 300 nm layer of silicon dioxide (SUMCO, JP) by the mechanical exfoliation method.¹ In detail, the silicon wafer was annealed at 200°C for 30 min and then cooled down until 70°C. Afterward, graphite or molybdenite (MoS₂) materials were exfoliated by using scotch tape and transferred to the silicon wafer at 70°C by sticking the tape against it. The tape was kept stuck to the silicon substrate for 15 s and removed carefully. In parallel, the Y4Y peptide was dissolved in distilled H₂O at concentrations of 10 nM and 100 nM of Y4Y. Then, a droplet of 100 μ L of each Y4Y solution was incubated on the fresh graphite/silicon and MoS₂/silicon substrates in a humid chamber at room temperature (25°C) for 1 hour according to Li et al.² A humid chamber was prepared for each experiment. For the self-assembly of Y4Y under 50% MeOH incubation, we dissolved Y4Y in water at 500 nM and then mixed it with MeOH to obtain the final concentration of 50% MeOH and 100 nM of Y4Y peptide.

AFM Image Processing.

To analyze the AFM images, we employed the image processing software Gwyddion (Czech Metrology Institute, CZ). In detail, we removed the tilt of surfaces and fixed the surface of substrates to 0 nm height. For estimation of the peptide coverage (to be understood as the percentage of area covered by the self-assembled structure formed on the substrate over the non-covered area), height information of peptide self-assembled structure was acquired as a profile of height distribution, which was deconvoluted with a bi-modal distribution of Gaussian model by using MATLAB (The MathWorks, Inc., USA). In height distribution profiles, a Gaussian peak at the lowest position was attributed to the height of substrate, and peaks showing larger height were assigned as the height distribution of peptide structures. The coverage of peptide nanostructures was determined by calculating the percentage of the peak area of peptide nanostructures over the total area of the height distribution curve (Fig. S3). After deconvolution of the peaks in the height distribution, the full-width half maximum (FWHM) was obtained from the peak corresponding to the self-assembled peptide Y4Y.

Fluorescence characterization

The samples were prepared by mixing thioflavin (ThT) with dissolved in 50% of organic solvent (for a final concentration of 10 μM of ThT and two concentrations of Y4Y 1 μM and 10 μM). The measurements were obtained at the initial mixing (0 min) with organic solvent and after 60 min of mixing.

The excitation wavelength of the device was set at 450 nm, and the spectra were recorded between 460 to 560 nm, detecting an emission peak between 485 to 490 nm depending on the employed organic solvent. The sampling pitch was 0.5 nm, and the size of the slits was 10 nm. A speed of sampling of 300 nm/min was employed to maintain a good signal-to-noise ratio. All the measurements were performed on the RF-6000 Shimadzu Spectrofluorometer® by using a four walls-clear quartz cell.

Contact angle measurement

The contact angle measurements were performed with SImage High-speed contact angle meter® by placing a droplet of 3 μL (typically less than 10 μL to avoid the influence of gravity) on the HOPG flat surface. Binary solutions of 50% vol/vol of organic solvents MeOH, EtOH, 1-prop, IPA, DMSO, and acetone were evaluated.

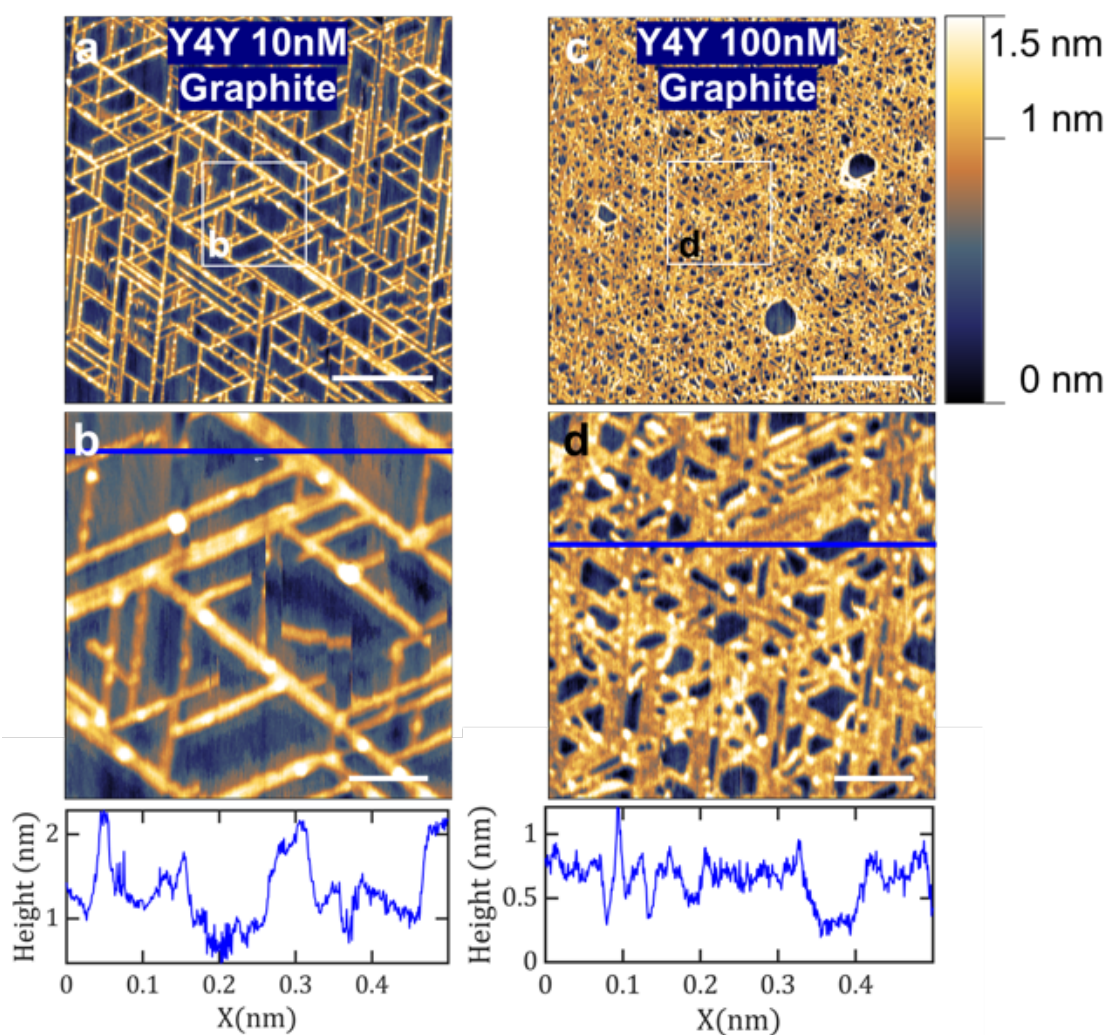


Figure S1. Self-assembly of Y4Y peptide on graphite. The self-assembly on graphite was obtained by incubating a droplet of 10 nM (a) and 100 nM (c) of Y4Y dissolved in DI water. The scale bar is 500 nm. (b) and (d) are the magnified images of the white sections in (a) and (c), respectively; underneath the line profiles at the blue line of the AFM images are shown. The scale bar is 100 nm.

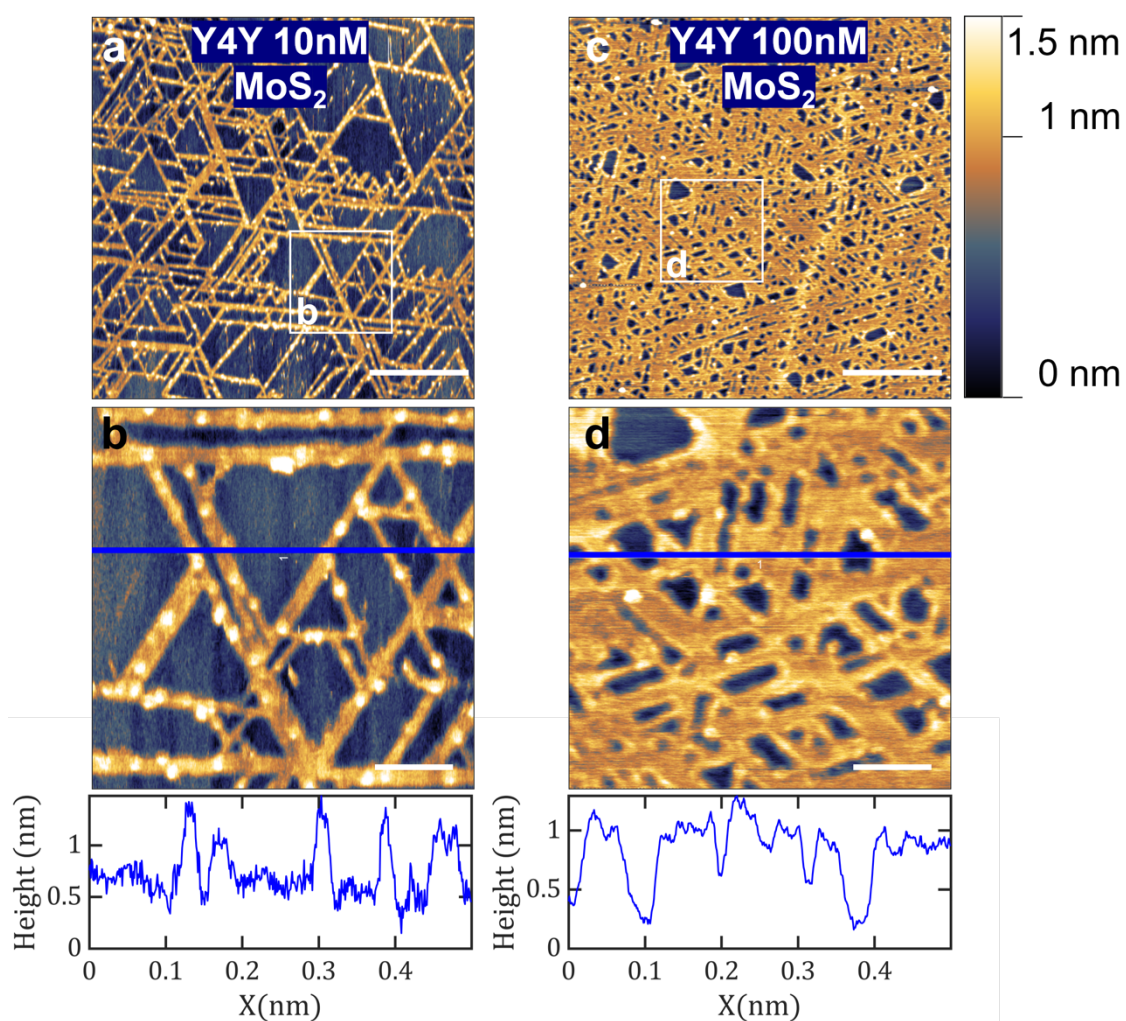


Figure S2. Self-assembly of Y4Y peptide on MoS₂. The self-assembly on MoS₂ was obtained by incubating a droplet of 10 nM (a) and 100 nM (c) of Y4Y dissolved in DI water. The scale bar is 500 nm. (b) and (d) are magnified images of the white sections in (a) and (c), respectively; underneath the line profiles at the blue line of the AFM images are shown. The scale bar is 100 nm.

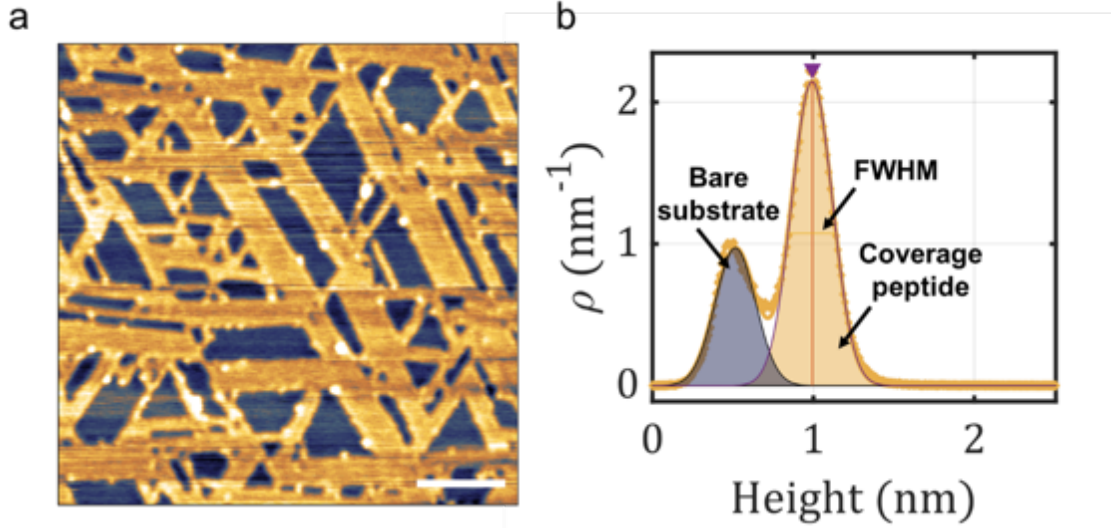


Figure S3. The method to estimate the coverage and the FWHM of the self-assembled structure on the surface. (a) An AFM image as an example: self-assembly of Y4Y peptide on MoS₂ after 1 hour of incubation under 10% MeOH. (b) the fitting of the height histogram corresponding to the image in (a), where the blue area is the coverage of the bare surface and the yellow area is the peptide coverage. FWHM was calculated from the peak corresponding to the peptide structure (Yellow). The scale bar is 100 nm.

For the estimation of the coverage, we employed a gaussian fitting by using the MATLAB software. The following equation was employed for fitting:

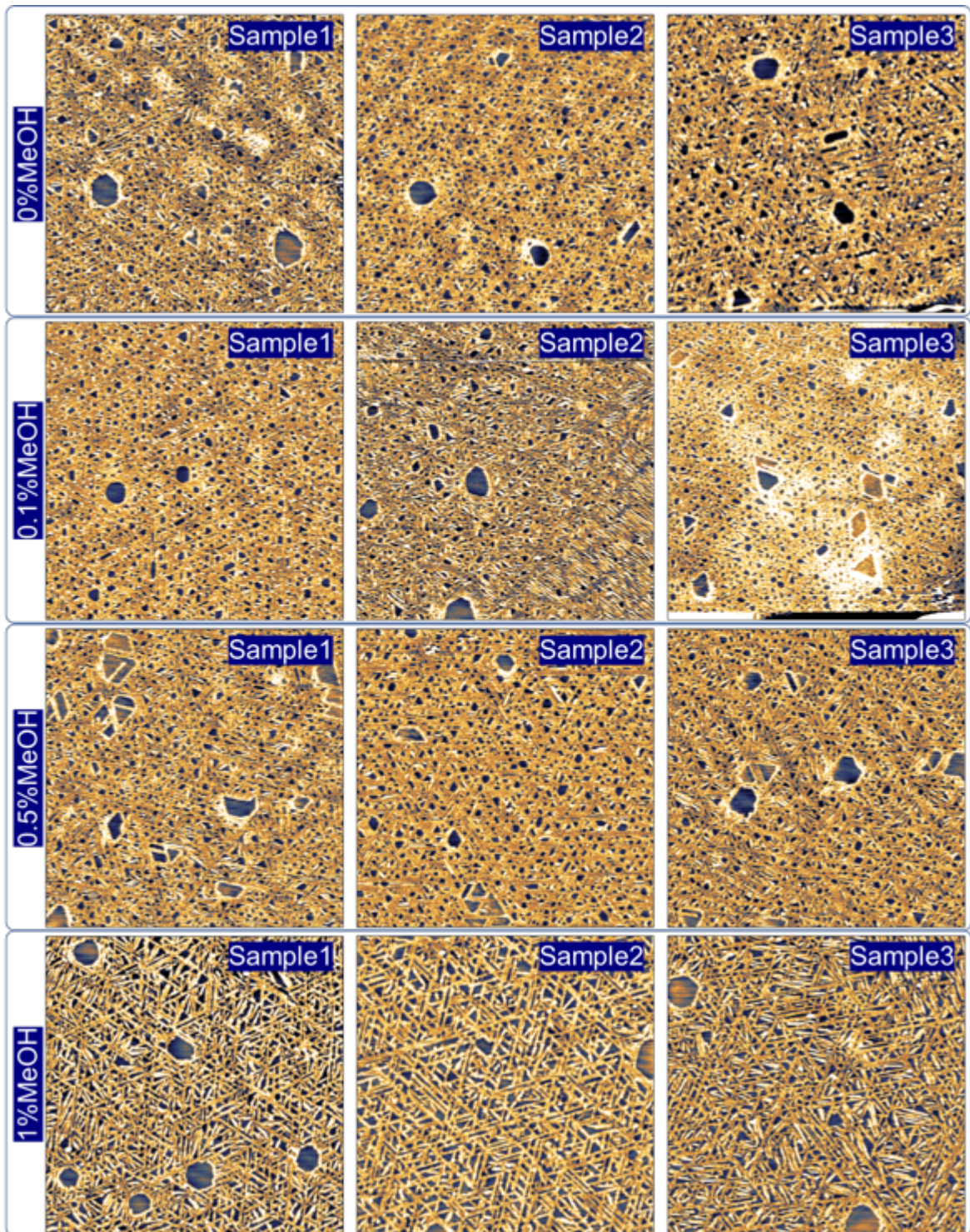
$$y = f(x) = \sum_{i=1}^n a_i e^{\left[-\left(\frac{x-b_i}{c_i}\right)^2\right]},$$

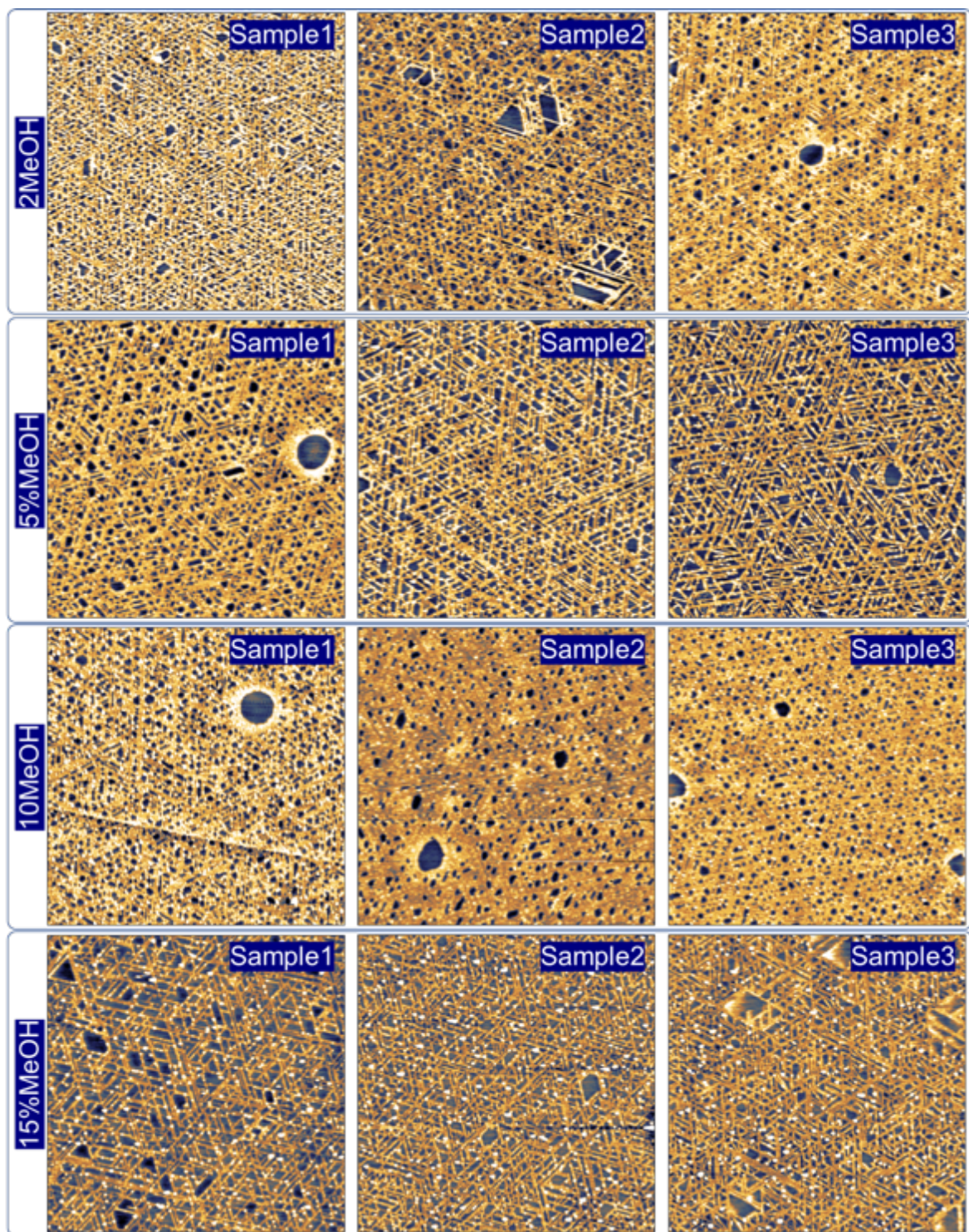
where a is the amplitude of the curve, b is the position of the peak, c is related to the peak width, and n is the number of peaks to fit.

For the deconvolution of two peaks, we employed the following equation:

$$y = f(x) = a_1 e^{\left[-\left(\frac{x-b_1}{c_1}\right)^2\right]} + a_2 e^{\left[-\left(\frac{x-b_2}{c_2}\right)^2\right]},$$

where the first term belongs to the fitting of the peak corresponding to the bare surface and the second term belongs to the peak corresponding to the self-assembled structure of Y4Y peptide.





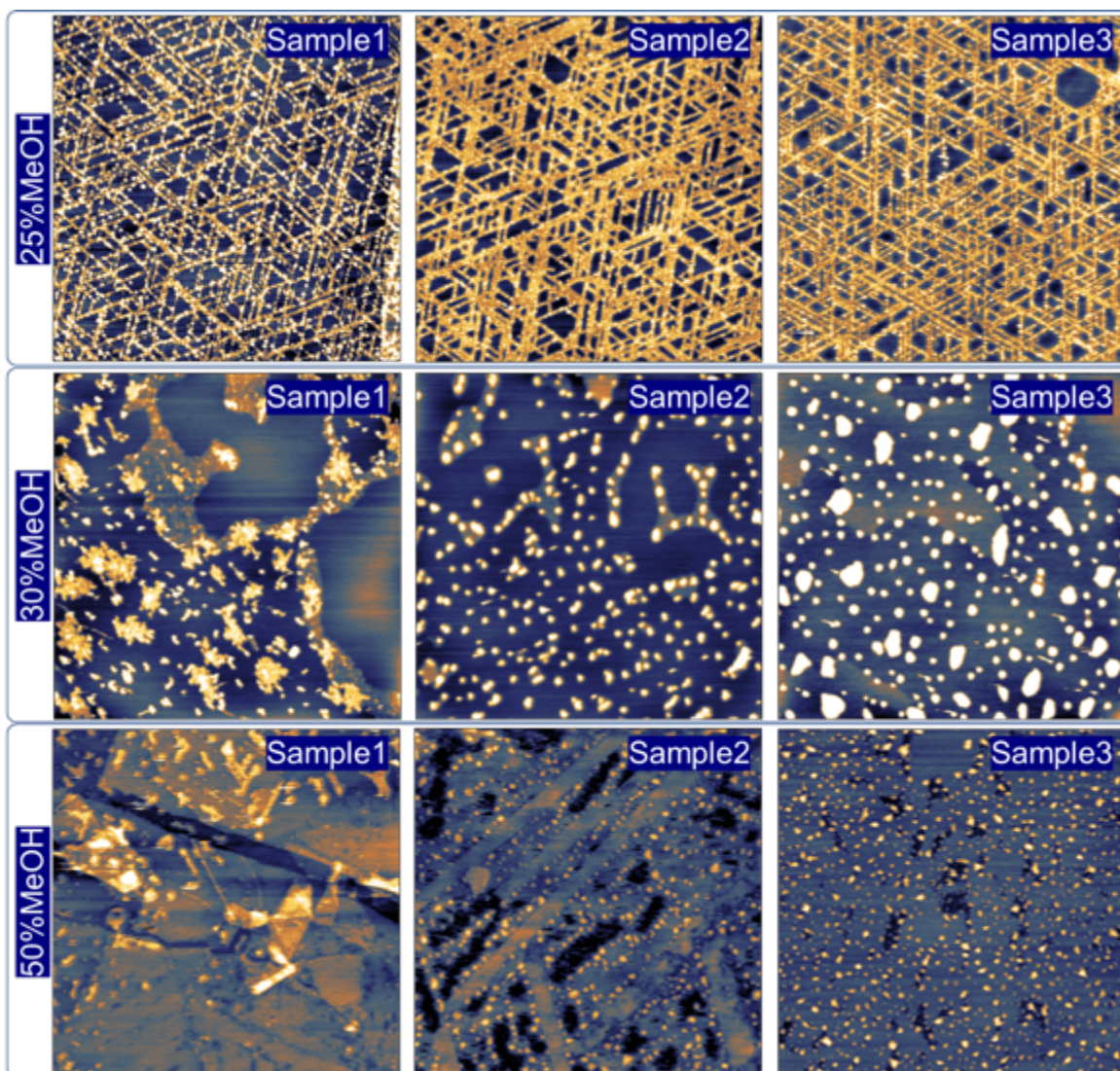
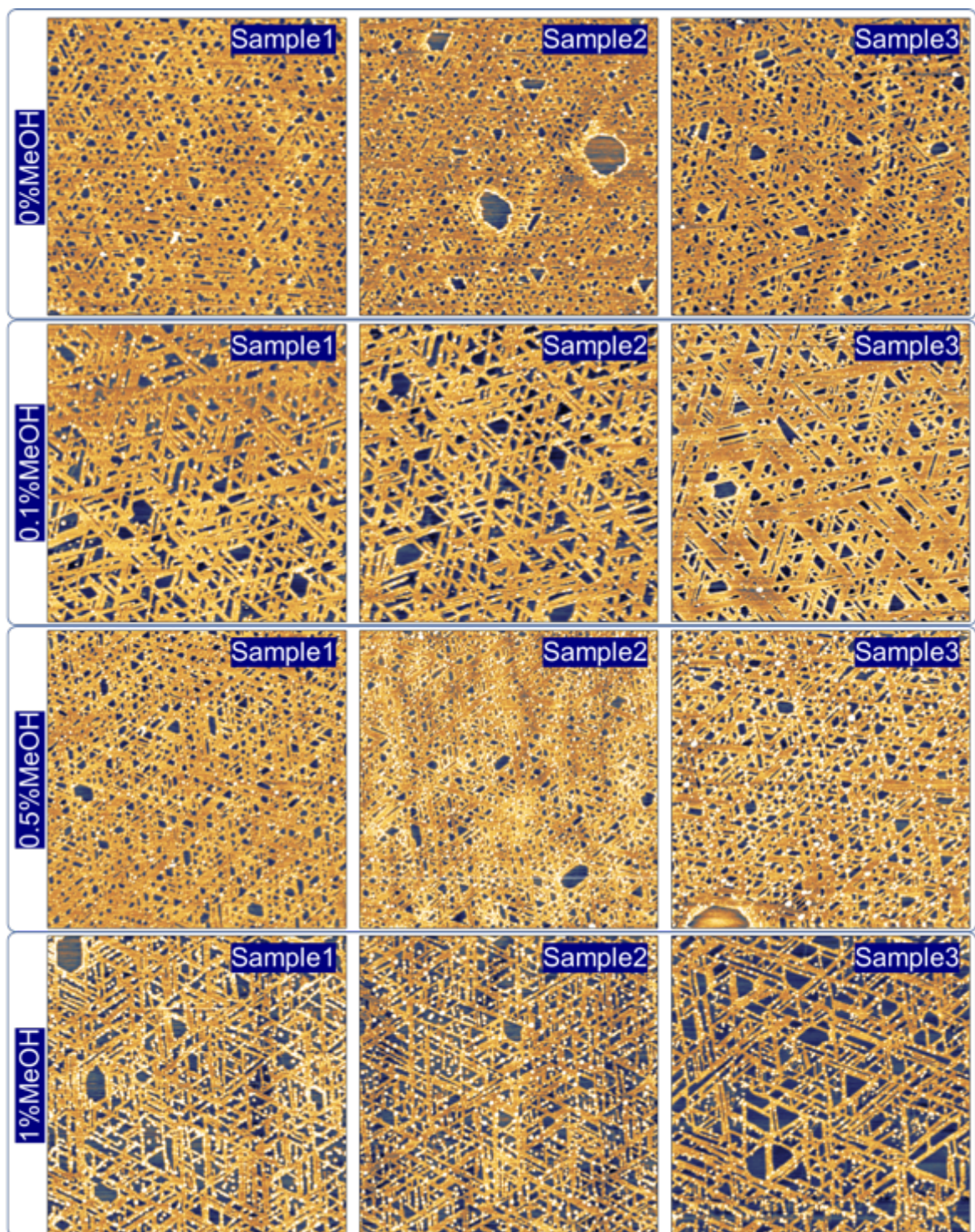
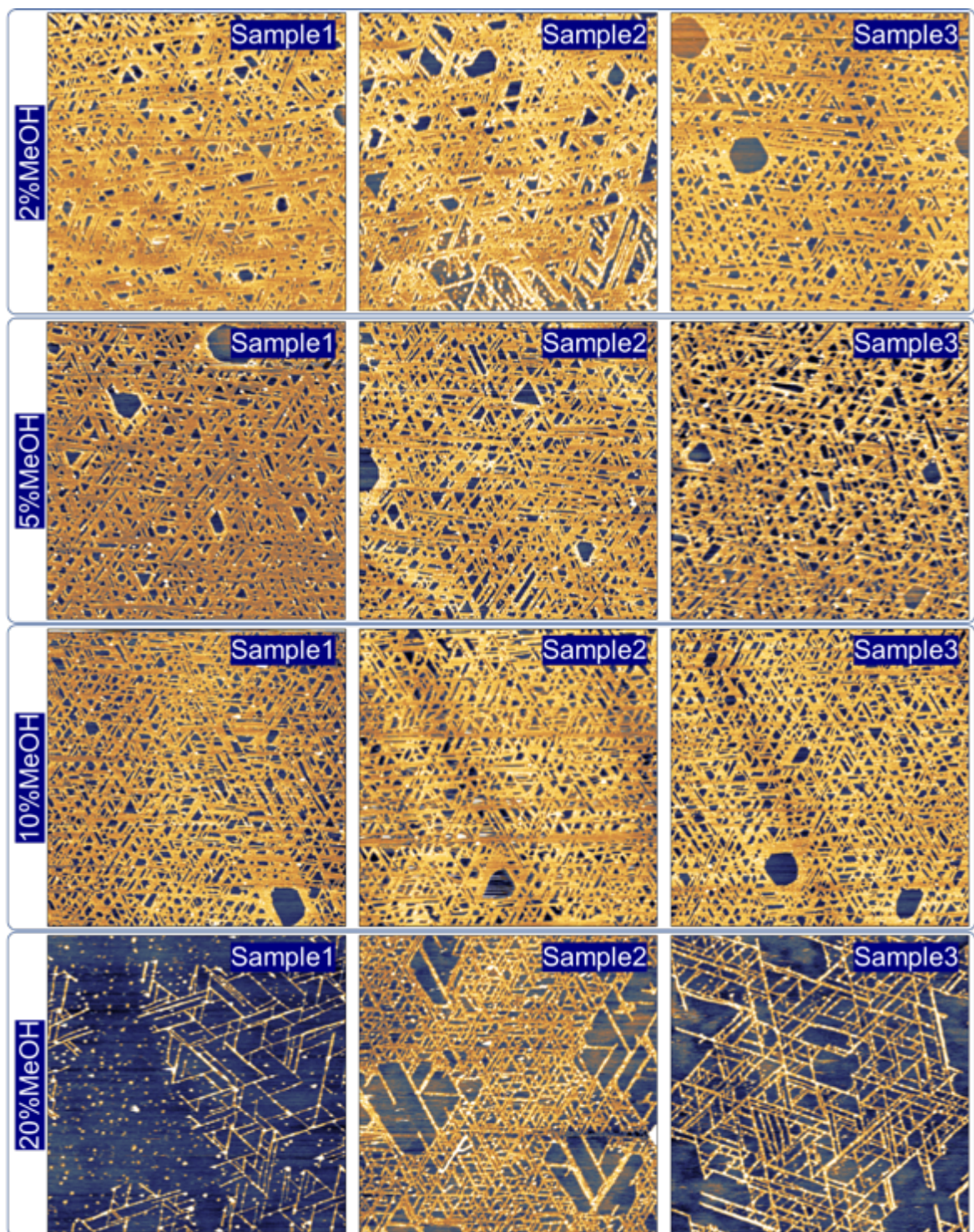


Figure S4. Self-assembly of Y4Y peptides on graphite under various concentrations of MeOH in DI water. Each row indicates the concentration of MeOH. All the AFM images were obtained from three different samples (sample1, sample2, and sample3). The size of AFM images is 2 x 2 μm .





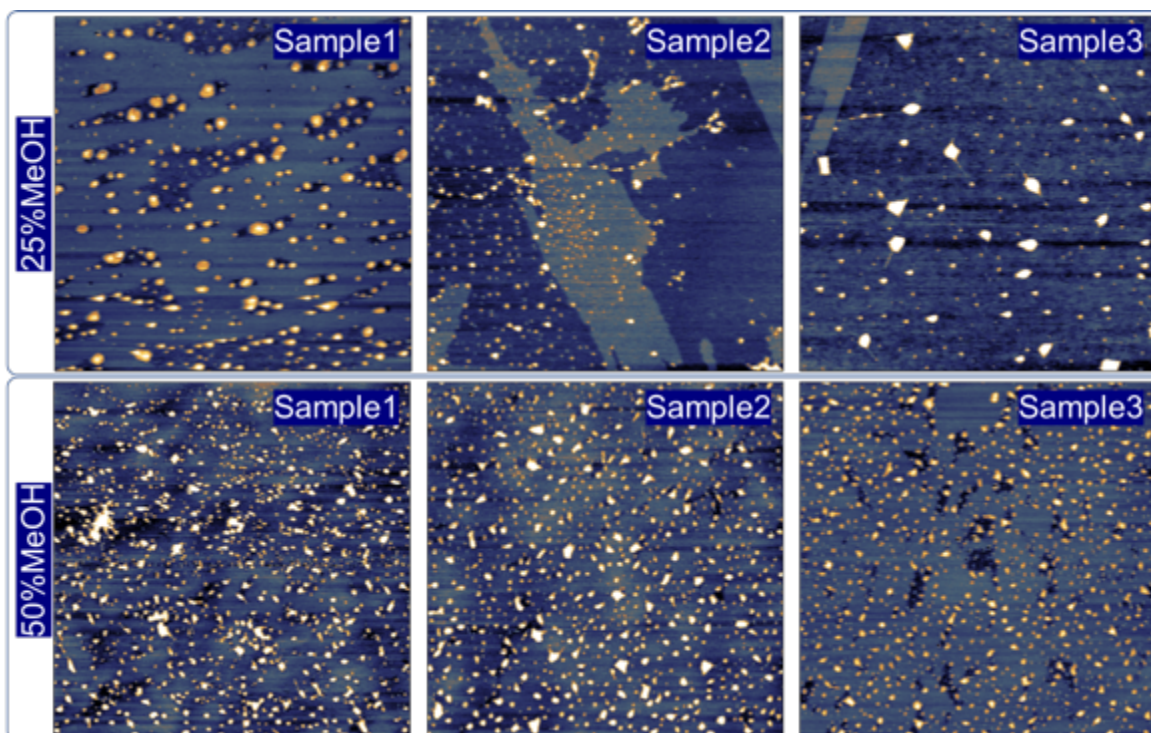


Figure S5. Self-assembly of Y4Y peptides on MoS₂ under various concentrations of MeOH in DI water. Each row indicates the concentration of MeOH. All the AFM images were obtained from three different samples (sample1, sample2, and sample3). The size of AFM images is 2 x 2 μm^2 .

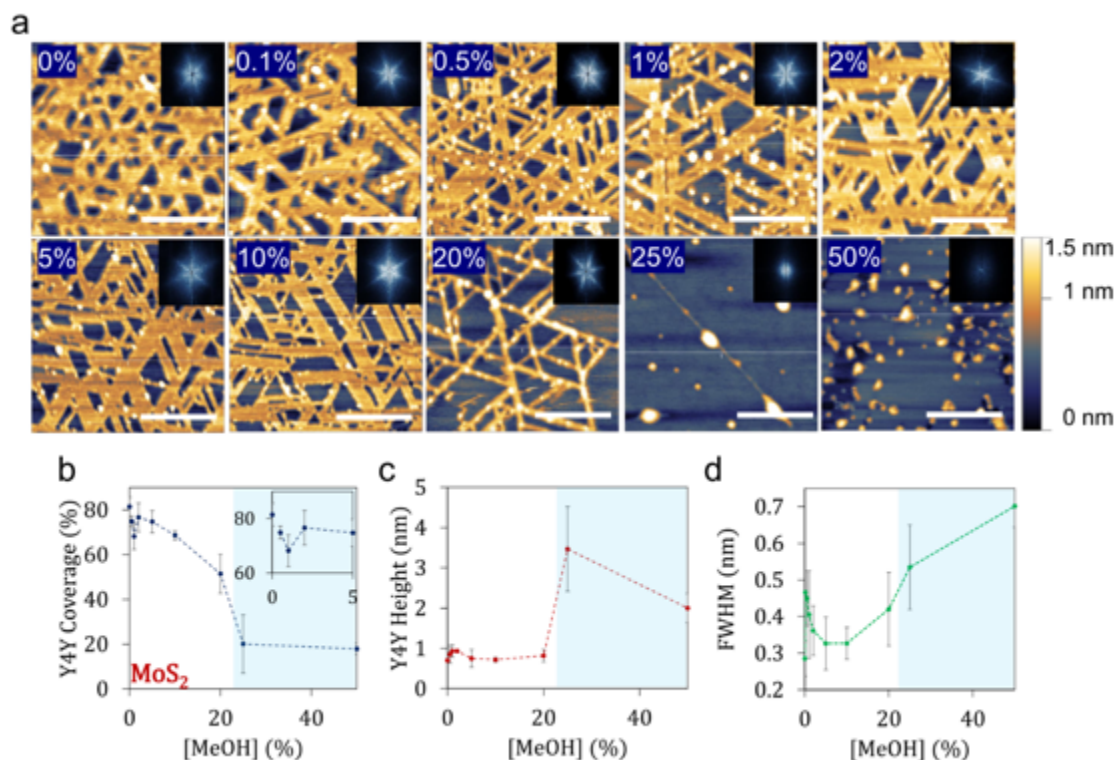


Figure S6. Self-assembly of Y4Y peptides on MoS₂ depending on the concentrations of MeOH. (a) AFM images of Y4Y self-assembled on MoS₂ under distinct concentrations of MeOH in DI water (ranging MeOH concentrations from left to right, top: 0 to 2%, bottom: 5 to 50%). The scale bar is 200 nm. (b) The surface coverage of Y4Y peptides depending on the concentration of MeOH. The inset shows an extended section of the plot from 0 to 5% of MeOH. (c) Y4Y peptide height depending on the concentration of MeOH. (d) FWHM of the peptide height distribution obtained per each AFM image and plotted according to the concentration of MeOH.

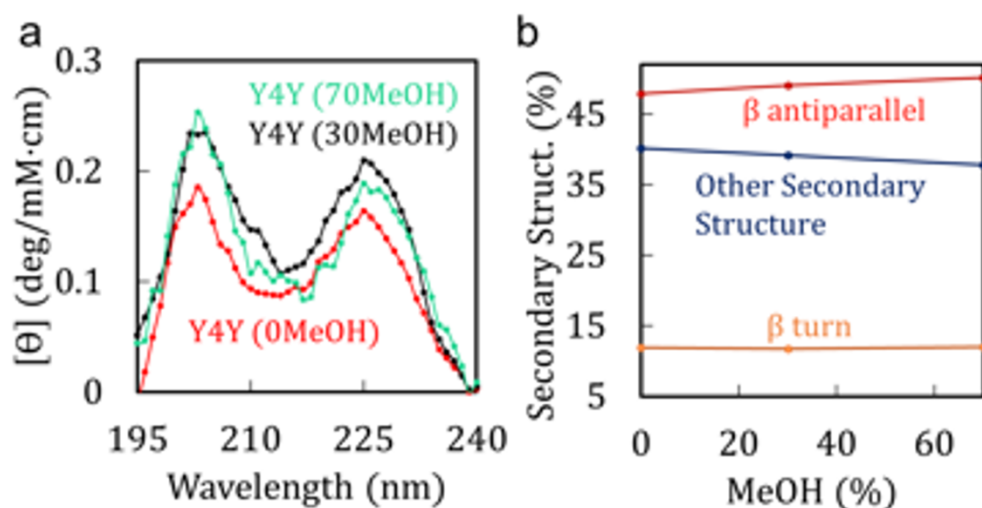


Figure S7. CD spectroscopy of Y4Y peptide. (a) CD curves of 100- μ M Y4Y peptide in co-solvents of 0%MeOH, 30%MeOH, and 70%MeOH in DI water. (b) Prediction of the percentage of Y4Y secondary structures upon the concentration of MeOH.

Circular Dichroism (CD) spectroscopy interpretation

We employed CD spectroscopy of Y4Y to evaluate the influence of organic solvent to investigate their possible aggregations. CD spectroscopy was performed to characterize the peptide structure in methanol-containing solutions. Peptide solutions in the co-solvents were prepared from an aqueous stock solution that contained a high concentration of peptide. According to the methanol needed in the solution, fresh samples were prepared just before the measurement by mixing methanol and stock aqueous solutions of the peptide. This procedure follows similar conditions as the droplet incubation process of peptides on surfaces. The solution was filled in a quartz cell (optical path length = 0.2 cm) and measured in the range of 190 to 250 nm. The characterization of the samples was performed by the Jasco CD spectrophotometer model J-1100 under the inert N_2 gas flow at a constant rate. The concentration of peptides used for this experiment was 100 μ M to obtain detectable signals, which was a thousand times larger than the one for peptide assembly on the surface.

Figure S7a shows spectra obtained for Y4Y dissolved in water, 30% and 70% MeOH. The peak ranging from 196 to 200 nm was attributed to the amount of β -sheet structures.³ The CD spectra did not show a significant change depending on the concentrations of MeOH. It suggests that peptide conformations were not altered by MeOH. The CD spectrum of peptide Y4Y presented a positive band at 216 nm and at 225 nm, suggesting an antiparallel relaxed β -sheet⁴.

The prediction and interpretation of β -sheet-rich peptides and proteins have proven to be difficult and biased due to their spectral variety, morphological and spectral diversity of the β structures, and the low spectral amplitudes.^{3–5} Due to this intrinsic limitation of the interpretation, we evaluated the increase of the β secondary structure regarding the

increment of methanol via a structure estimation by BeStSel software (Fig. S7b).⁴ Micsonai et al.⁴ proposed distinct CD patterns based on twist angle between two strands of the antiparallel β -sheet secondary structure. For the β -sheet formed with a slightly right-hand twist angle between two strands, the CD spectra have a similar pattern to the Y4Y peptide result. According to this consideration to classify the antiparallel β -sheet, we estimated the secondary structure. This estimation determined that methanol in solution does not affect the amount of the β -sheet secondary structure depending on the MeOH concentration. In addition, the blue curve shows that the percentage of other secondary structures different from α and β is also insensitive to the concentration of MeOH. Besides, the β -turns are estimated to be present at $\sim 12\%$, and there is no drastic change depending on the MeOH concentration.

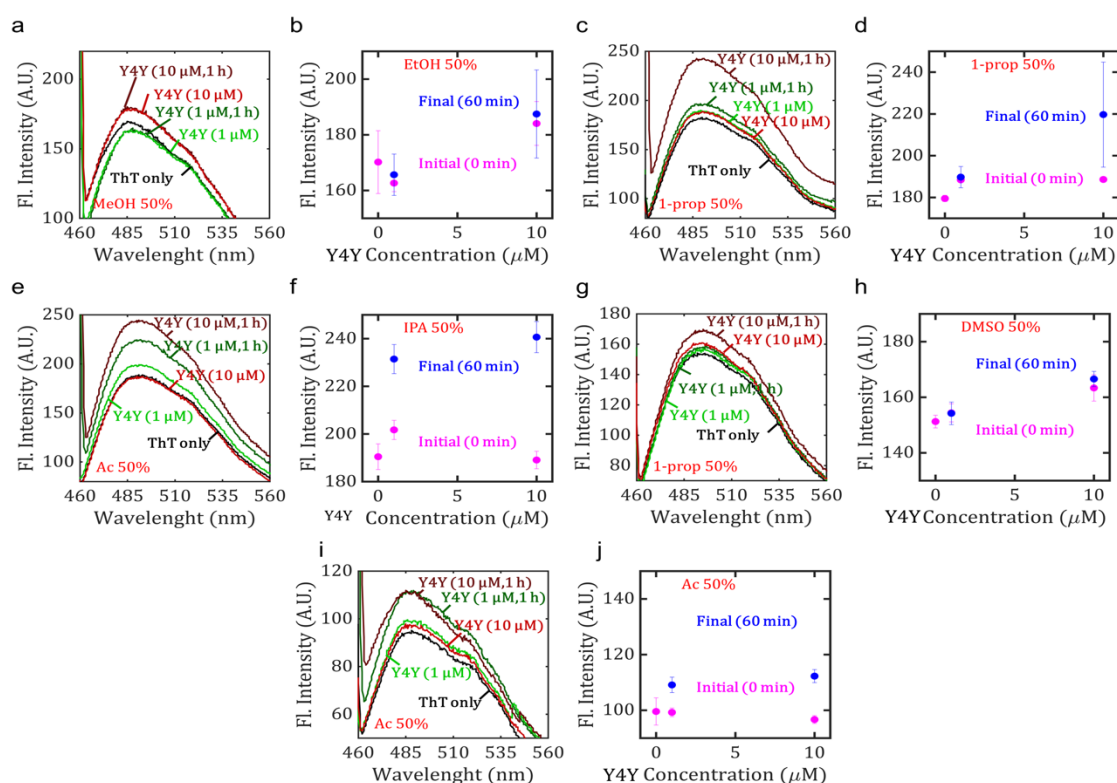


Figure S8. Fluorescence intensity spectra and fluorescence intensity average of ThT/Y4Y at the initial mixture in organic solvent and after 1 h in a solution of 50% EtOH (a,b), 50% 1-prop (c,d), 50% IPA (e,f), 50% DMSO (g,h) and 50% acetone (i,j). Fluorescence intensity average of ThT/Y4Y over distinct concentrations of Y4Y and at the initial mixture with MeOH and after one hour in a solution of 50% MeOH.

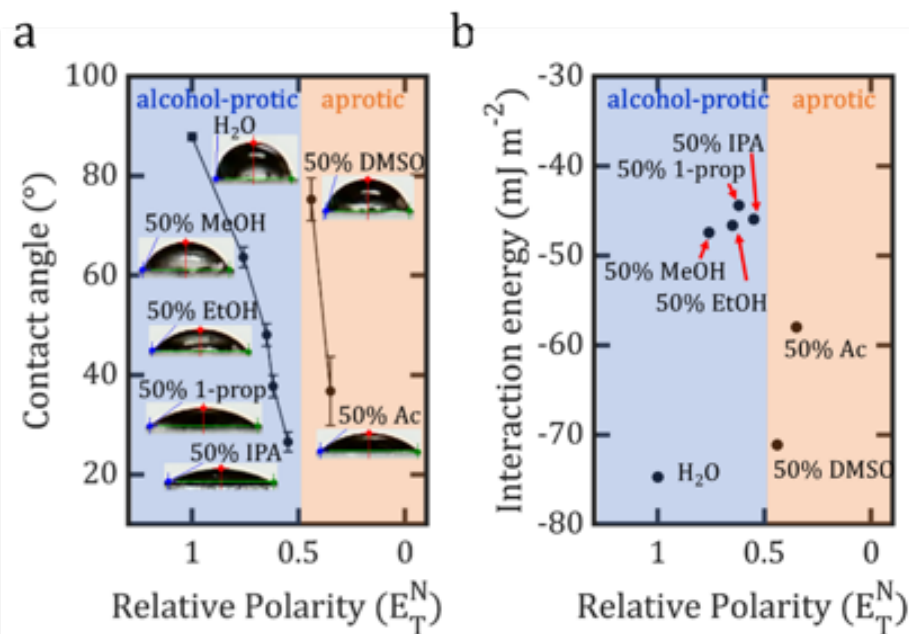


Figure S9. (a) Contact angle measurements of water and solutions containing 50% vol/vol of organic solvents MeOH, EtOH, 1-prop, IPA, DMSO, and acetone on HOPG. (b) Interaction potential energy of co-solvents on HOPG surface. The relative polarity of each solvent was obtained from a reference.⁶

To support the finding in the main text, we performed contact angle measurements, which provide information on the wetting of each co-solvent to the HOPG surface. Figure S11 shows the contact angle and the calculated van der Waals interaction potential energy⁷ (also defined as an adhesion work, which means a reversible thermodynamic work required to separate the interface from the equilibrium state of two phases to independently separated two phases) between the co-solvates and HOPG surface. The co-solvents with alcohol-protic solvent showed higher interaction energy with values between -45 to -48 mJ m^{-2} in contrast to the lower interaction energy of water that was -75 mJ m^{-2} . Regarding the aprotic solvents, DMSO and acetone showed interaction energy of -72 and -58 mJ m^{-2} , respectively. The higher interaction potential energy of the binary solutions in contrast to distilled water suggests that organic solvents have a preference to wet the surface of HOPG.

To calculate the van der Waals interaction potential energy, we employed the Young-Dupré equation as it is expressed:

$$\gamma_L(1 + \cos \theta) = -\Phi,$$

where γ_L is the surface tension of the liquid, θ is the contact angle, and Φ is the interaction potential energy per unit area between the liquid droplet and surface of HOPG⁸. The surface tensions of the binary liquids were obtained from Vazquez et al.⁹, Markarian et al.¹⁰, and Enders et al.¹¹.

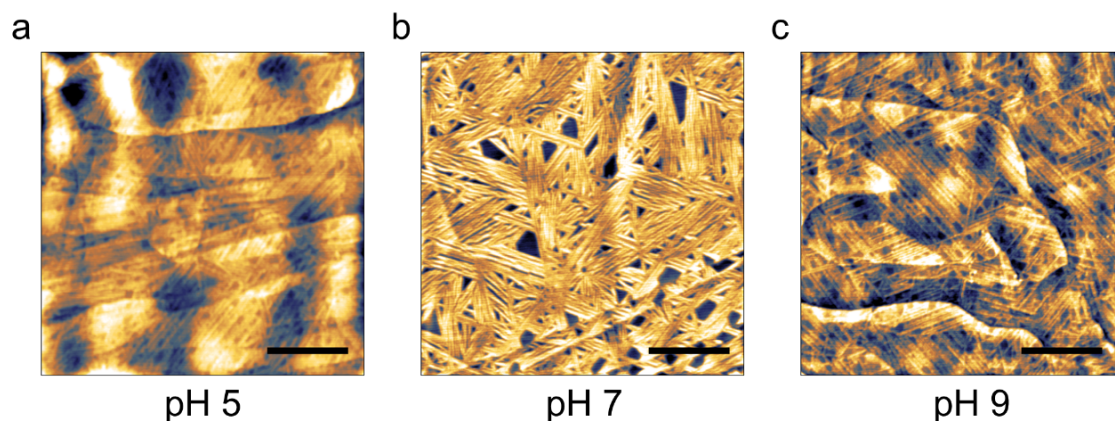


Figure S10. AFM images of self-assembled Y4Y after incubation when the aqueous medium was adjusted to pH 5 (a), pH 7 (b), and pH 9 (c) by using HCl and NaCl. Scale bar: 500nm.

References

- (1) Novoselov, K. S.; Geim, A. K.; Morozov, S. V.; Jiang, D.; Zhang, Y.; Dubonos, S. V.; Grigorieva, I. V.; Firsov, A. A. Electric Field in Atomically Thin Carbon Films. *Science* (80-.). **2004**, *306* (5696), 666–669. <https://doi.org/10.1126/science.1102896>.
- (2) Li, P.; Sakuma, K.; Tsuchiya, S.; Sun, L.; Hayamizu, Y. Fibroin-like Peptides Self-Assembling on Two-Dimensional Materials as a Molecular Scaffold for Potential Biosensing. *ACS Appl. Mater. Interfaces* **2019**, *11* (23), 20670–20677. <https://doi.org/10.1021/acsami.9b04079>.
- (3) Greenfield, N. J. Using Circular Dichroism Spectra to Estimate Protein Secondary Structure. *Nat. Protoc.* **2007**, *1* (6), 2876–2890. <https://doi.org/10.1038/nprot.2006.202>.
- (4) Micsonai, A.; Wien, F.; Kernya, L.; Lee, Y. H.; Goto, Y.; Réfrégiers, M.; Kardos, J. Accurate Secondary Structure Prediction and Fold Recognition for Circular Dichroism Spectroscopy. *Proc. Natl. Acad. Sci. U. S. A.* **2015**, *112* (24), E3095–E3103. <https://doi.org/10.1073/pnas.1500851112>.
- (5) Khrapunov, S. Circular Dichroism Spectroscopy Has Intrinsic Limitations for Protein Secondary Structure Analysis. *Anal. Biochem.* **2009**, *389* (2), 174–176. <https://doi.org/10.1016/j.ab.2009.03.036>.
- (6) Reichardt, C.; Eds, A. *Solvents and Solvent Effects in Organic Chemistry*, fourth.; Wiley-VCH: Germany, 2011. <https://doi.org/10.1002/9783527632220>.
- (7) Deville, J. P.; Cojocaru, C. S. Spectroscopic Analyses of Surfaces and Thin Films. In *Materials Surface Processing by Directed Energy Techniques*; Elsevier Inc., 2006; pp 411–441. <https://doi.org/10.1016/B978-008044496-3/50013-7>.

- (8) Shih, C. J.; Wang, Q. H.; Lin, S.; Park, K. C.; Jin, Z.; Strano, M. S.; Blankschtein, D. Breakdown in the Wetting Transparency of Graphene. *Phys. Rev. Lett.* **2012**, *109* (17), 1–5. <https://doi.org/10.1103/PhysRevLett.109.176101>.
- (9) Vazquez, G.; Alvarez, E.; Navaza, J. M. Surface Tension of Alcohol + Water from 20 to 50 °C. *J. Chem. Eng. Data* **1995**, *40* (3), 611–614. <https://doi.org/10.1021/je00019a016>.
- (10) Markarian, S. A.; Terzyan, A. M. Surface Tension and Refractive Index of Dialkylsulfoxide + Water Mixtures at Several Temperatures. *J. Chem. Eng. Data* **2007**, *52* (5), 1704–1709. <https://doi.org/10.1021/je7001013>.
- (11) Enders, S.; Kahl, H.; Winkelmann, J. Surface Tension of the Ternary System Water + Acetone + Toluene. *J. Chem. Eng. Data* **2007**, *52* (3), 1072–1079. <https://doi.org/10.1021/je7000182>.